This is the accepted manuscript made available via CHORUS. The article has been published as:

Abruptly autofocusing and autodefocusing optical beams with arbitrary caustics

Ioannis D. Chremmos, Zhigang Chen, Demetrios N. Christodoulides, and Nikolaos K. Efremidis

Phys. Rev. A **85**, 023828 — Published 22 February 2012

DOI: 10.1103/PhysRevA.85.023828

Abruptly autofocusing and autodefocusing optical beams with arbitrary caustics

Ioannis D. Chremmos[1], Zhigang Chen[2], Demetrios N. Christodoulides[3], and Nikolaos K. Efremidis[1]

[1] Department of Applied Mathematics, University of Crete, Heraklion 71409, Crete, Greece

[2] Department of Physics and Astronomy, San Francisco State University, San Francisco, CA 94132

[3] CREOL/College of Optics, University of Central Florida, Orlando, Florida 32816

Corresponding author: jochremm@central.ntua.gr

Abstract: We propose a simple yet efficient method for generating abruptly autofocusing optical beams with arbitrary caustics. In addition we introduce a family of abruptly autodefocusing beams whose maximum intensity suddenly decreases by orders of magnitude right after the target. The method relies on appropriately modulating the phase of a circularly symmetric optical wavefront, such as that of a Gaussian, and subsequently on Fourier-transforming it by means of a lens. If two such beams are superimposed in a Bessel-like standing wave pattern, then a complete mirror-symmetric, with respect to the focal plane, caustic surface of revolution is formed that can be used as an optical bottle. We also show how the same method can be used to produce accelerating 1D or 2D optical beams with arbitrary convex caustics.

1. Introduction

Recently, a family of optical waves was introduced with abruptly autofocusing (AAF) properties [1]. The new waves (also termed circular Airy beams - CAB) have a circularly symmetric initial amplitude that oscillates outward of a dark disk like an exponentially truncated Airy function. By virtue of the two outstanding features of finite-power Airy beams [2,3], namely their self acceleration and their resistance to diffraction, this eventually results in light beams, that can propagate over several Rayleigh lengths with minimum shape distortion and almost constant maximum intensity, until an abrupt focusing takes place right before a target, where the intensity is suddenly enhanced by orders of magnitude. These theoretical predictions were subsequently verified by experimental observations [4,5]. These observations also demonstrated that AAF beams could outperform standard Gaussian beams, especially in settings where high intensity contrasts must be delivered under conditions involving long focal-distance-to-aperture ratios (f-numbers) [4]. In addition, this "silent" or low intensity mode, at which AAF waves approach their target, makes them ideal candidates for medical laser applications where collateral tissue damage is supposed to be kept at a minimum. Other possible applications include laser waveguide writing in bulk glasses and particle trapping and guiding [5].

The focusing mechanism of AAF beams is fundamentally different from that of Gaussian beams. In the latter case, the wave's constituent rays form a sharpened pencil that converges at a single point, the focus. As the beam's cross-sectional area gradually decreases, the maximum intensity over the transverse plane increases in a Lorentzian fashion, centered at the focus. In the case of AAF beams however, the rays responsible for focusing are emitted from the exterior of a dark disk on the input plane and stay tangent to a convex caustic surface of revolution (SoR) that contracts toward the beam axis [1]. By virtue of its Airy transverse amplitude profile, this caustic is intrinsically diffraction-resisting, therefore keeping its maximum intensity almost constant during propagation and its interior almost void of optical energy. Focusing occurs as a result of an on-axis collapse of this SoR and is so abrupt as the transition from the dark to the lit side of an optical caustic. At the point of 'collapse', the rays emitted from a certain circle on the input plane interfere constructively and the gradient of the field amplitude is maximized.

Building on the concept of a collapsing caustic SoR, the AAF wave family was recently broadened to include general power-law caustics that evolve from a sub-linearly chirped input amplitude [6]. In this latter work, we showed that a ν^{th}-power caustic requires the input amplitude to oscillate with a chirp of the order $\beta = 2 - \nu^{-1}$, which generalizes the case of CABs, whose parabolic trajectory is a result of the $3/2$ chirp of the Airy function itself. Although not non-diffracting as ideal CABs, these *pre-engineered* beams were shown to exhibit attractive features, such as enhanced focusing abruptness, larger intensity contrasts and suppressed post-focal intensity maxima.

To benefit from the attractive properties of AAF waves, it is crucial to generate them efficiently. This is generally a nontrivial task, since these waves evolve from initial amplitudes that are not easy to implement directly, such as concentric Airy rings. A possible alternative is to generate the Fourier transform (FT) of the initial condition first and then inverse-Fourier transform it by means of a lens. A similar approach was adopted in the first demonstration of CABs [4], where the initial wavefront was produced by encoding both amplitude and phase information on a phase-only filter. The FT technique was also employed in [7], where a hologram of the FT was produced. In addition in this latter work, the FT of CABs was treated analytically and found to behave like a Bessel function whose argument is enhanced by a cubic phase term, i.e. a quadratic chirp. By tuning the strength of the chirp relative to the lens' focal distance, it was possible to generate AAF beams with two foci, the one being defocusing while the other one focusing, thereby defining the ends of an elegant paraboloid optical bottle [7].

From the above it is clear that producing AAF beams can be equally difficult, either in the real or in the Fourier space, since, in both cases, a complicated initial condition, varying both in phase and in amplitude, must be produced. However, when the requirement for the exact generation of a specific AAF wave can be relaxed, the implementation procedure can be significantly simplified. Indeed, having explained the AAF mechanism through both ray and wave optics [1,6], one realizes that the critical phenomenon is the formation of the caustic and depends primarily on the phase modulation of the input wavefront and secondarily on the envelope of its amplitude. This fact has already facilitated the generation of arbitrary convex 1D or 2D beams, by applying the appropriate 1D or 2D phase mask on a plane wave [9] or

on a Gaussian beam [10]. This is perhaps the most obvious way to directly produce accelerating 1D or 2D caustics. However, in some applications, it could be more advantageous to apply the same concept in the Fourier space. A major reason is that the FT lens provides an additional degree of freedom for easily *targeting* and *sizing* the generated beam [7]. Indeed, as noted in the latter paper, the optical bottles produced with the FT method can be arbitrarily scaled without losing their symmetry or having to modify the input condition, by simply changing the lens' focal distance. This is a true advantage of the FT approach compared to the direct (real-space) approach, which requires that all beam characteristics must be prescribed on the phase mask, while even a simple scaling of the beam requires to redesign the phase modulation. In addition, the lens offers a physical $2f$ separation between object and image planes, which could be useful in applications when the phase mask cannot be positioned very close to the target.

In this work, we present a simple yet general method for generating in the Fourier space AAF or abruptly autodefocusing (AADF) optical beams with pre-engineered caustic SoR. From a certain viewpoint, this generalizes our previous work on CABs and their parabolic caustics [7] to AAF waves with arbitrary convex caustics. We hereby show that such beams can be produced efficiently by simple means of a circularly symmetric phase mask and a FT lens, acting successively on an optical wavefront with no particular amplitude information. The required phase is the sum of a linear and a nonlinear term. The linear term is responsible for creating an annular focusing pattern on the image plane, while the nonlinear term is responsible for transforming this pattern into an Airy pattern thus determining the shape of the caustic produced before or after that plane. Special attention is paid to the case of power-law caustics, for which analytical results are readily obtained and reported. In particular, we find that a ν^{th}-power caustic requires a n^{th}-power phase with the orders being related as $n=(2\nu-1)/(\nu-1)$. Counter-intuitively, for a given ν, the stronger the nonlinear phase the weaker is the acceleration of the caustic, hence the longer is the distance from the image plane to the target. The linear phase and the lens' focal plane determine the size of the produced AAF beam in terms of its width at the image plane, and also in terms of the distance from that plane to the target.

In Section 2, we describe the proposed method analytically and subsequently, in Section 3, we support it with numerical calculations that demonstrate the

generation of AAF and AADF beams and also that of optical bottles with sinusoidal shape. Although our focus is on AAF waves, we complete this paper by showing that the same method can actually be used to produce accelerating 1D or 2D beams with arbitrary convex trajectories.

2. Engineering AAF/AADF waves in the Fourier space

To begin, consider the amplitude of a phase-modulated circularly symmetric wavefront

$$u_0(r) = A(r)\exp[i\Phi(r)] = A(r)\exp[iar + iq(r)], \tag{1}$$

where r is the polar distance normalized by an arbitrary length, say x_0, $A(r)$ is a real envelope and $\Phi(r)$ is the phase consisting of a linear term with slope $a > 0$ and a nonlinear (e.g. power-law) term $q(r)$. Such an initial condition can be easily realized by reflecting a plane wave or a collimated Gaussian beam on the face of a spatial light modulator (SLM) programmed with a phase $\Phi(r)$. Subsequently, let us examine the evolution of this wave through the single-lens FT system of Fig. 1 under the validity of the paraxial approximation $2u_z = i\nabla_t^2 u,$ where subscript t stands for *transverse* and z is the propagation distance normalized by $2\pi x_0^2/\lambda,$ λ being the optical wavelength. Propagating the waves before and after the lens according to the Fresnel diffraction integral [6], and taking into account the quadratic phase $\exp(-ir^2/2f)$ imprinted on the wave transmitted through the lens, it can be shown that the optical field on the image plane ($z = 2f,$ where f is the focal length) reads

$$u(r, z = 2f) = -(i/f)U_0(r/f), \tag{2}$$

where

$$U_0(k) = \int_0^\infty u_0(\rho) J_0(k\rho)\rho d\rho \tag{3}$$

is the Hankel transform of the object wavefunction $u_0(\rho)$. Obviously, Eq. (2) expresses the FT property of the lens. Substituting Eq. (3) into Eq. (2) and using the familiar integral representation of Bessel function

$$J_0(x)=\frac{1}{2\pi}\int_0^{2\pi}\exp(-ix\cos\varphi)\,d\varphi, \tag{4}$$

we obtain

$$u(r,z=2f)=-\frac{i}{2\pi f}\int_0^{\infty}\int_0^{2\pi}\mathrm{A}(\rho)\exp\left(ia\rho+iq(\rho)-i\frac{\rho r}{f}\cos\varphi\right)\rho\,d\rho\,d\varphi, \tag{5}$$

where u_0 was substituted from Eq. (1). Even in its simplified form of Eq. (3), this integral cannot be evaluated analytically for a general function $q(\rho)$. Hence it is reasonable to resort to a stationary-phase (SP) computation, which is justified by the oscillatory nature of the integrand. Assuming that $q'(\rho)>0$ for all $\rho>0,$ where the prime denotes the derivative with respect to the argument, it is readily seen that there is only one stationary point $(\rho_s,\varphi_s)=(r_0,0),$ where r_0 is the solution of equation

$$a+q'(r_0)=r/f. \tag{6}$$

After some algebra, the result of integration in the neighbourhood of (ρ_s,φ_s) is

$$u^{SP}(r,z=2f)=\sqrt{\frac{r_0}{fq''(r_0)r}}\mathrm{A}(r_0)\exp\left(iar_0+iq(r_0)-i\frac{r_0 r}{f}\right). \tag{7}$$

The last two equations lead to two important conclusions: First, Eq. (6) implies $r>af,$ which means in essence that only points on the image plane lying outside that disk plane have appreciable amplitude. Secondly, since r_0 is a function of the observation point *r*, Eq. (7) shows that the wave amplitude on the image plane is also nonlinearly phase-modulated. Differentiating the phase of Eq. (7) with respect to *r* and using Eq. (6), one obtains $-r_0/f<0,$ i.e. the phase modulation is of converging nature. Therefore, the wave on the image plane satisfies the preconditions for evolving into an AAF wave. If the phase of Eq. (7) is properly designed, then an inward bending caustic SoR with initial width $2af$ will be formed and eventually focus abruptly somewhere in the half-space $z>2f$.

Further understanding of this process can be gained through a ray optics interpretation of the propagation dynamics. Referring to Fig. 1, let us follow the path of the ray starting from point $(r_0,0)$ on the input plane. According to Eq. (1), this ray

travels at an angle θ_0 with the z-axis and reaches the surface of the lens (which is assumed to be infinitesimally thin) at $\left(r_1, f^-\right)$, where $r_1 = r_0 + fs_0$ and

$$s_0 \triangleq \tan\theta_0 = \Phi'(r_0) \tag{8}$$

is the corresponding slope. Passing through the lens, the ray deflects inwards and emerges from point $\left(r_1, f^+\right)$, with a modified slope $s_1 \triangleq \tan\theta_1 = s_0 - r_1 / f$. The transmitted ray crosses the image plane at $r_2 = r_1 + fs_1$ with a slope $\tan\theta_2 \triangleq s_2 = s_1$. Combining the above we obtain the equations

$$r_2 = fs_0, \qquad s_2 = -r_0 / f, \tag{9}$$

connecting the exit position and slope of a ray (r_2, s_2) to the input values (r_0, s_0). Equations (9) are equivalent to the conclusions reached previously, noting that the point here named r_2 is the observation point r of Eqs. (6) and (7). As $\left(r_0, s_0(r_0)\right)$ vary continuously along the input plane, the transmitted rays form a caustic that is expressed with coordinates (r_c, ξ_c), where r_c is the radial distance, $\xi_c = z - 2f$ is the distance from the image plane and (r_c, ξ_c) is interpreted as the point at which ray (r_2, s_2) touches the caustic. From Fig. 1 obvious are also the equations

$$s_2 = r_c'(\xi_c), \qquad r_c = r_2 + \xi_c s_2. \tag{10}$$

Differentiating the second of Eqs. (10) with respect to ξ_c and using Eqs. (9), it can be shown that the caustic is expressed in terms of the input ray characteristics as

$$(r_c, \xi_c) = \left(fs_0(r_0) - fr_0 s_0'(r_0), f^2 s_0'(r_0)\right), \tag{11}$$

where r_0 serves as a parameter and $s_0(r_0)$ is given by Eq. (8). Equations (8) and (11) provide the means for a direct design approach, namely to determine the caustic resulting from a given input phase modulation. Alternatively, one could work inversely and find the input ray parameters associated with a desired caustic $\left(r_c(\xi_c), \xi_c\right)$. Again from Eqs. (9) and (10) we obtain directly

$$(r_0, s_0) = \left(-f r_c'(\xi_c), \frac{1}{f}\left[r_c(\xi_c) - \xi_c r_c'(\xi_c) \right] \right) \tag{12}$$

where the parameter now is ξ_c. From Eqs. (12) it is evident that, for $r_c''(\xi_c) < 0$, i.e. for a convex caustic, we have $r_0'(\xi_c) > 0$, which ensures that the rays touching the caustic at different points do not overlap on the input plane. This allows us to invert function $r_0(\xi_c)$ and determine the phase $\Phi(r_0)$ associated with ray characteristics (r_0, s_0). Integrating Eq. (8) by introducing the new variable ξ_c one gets

$$\Phi(r_0) = \int_0^{\xi_c(r_0)} s_0(\xi) r_0'(\xi) d\xi = \int_0^{\xi_c(r_0)} \left[\xi r_c'(\xi) - r_c(\xi) \right] r_c''(\xi) d\xi \tag{13}$$

where $\xi_c(r_0)$ is the inverse of function $r_0(\xi_c)$, and functions $s_0(\xi), r_0(\xi)$ were obtained from Eqs. (12) by substituting ξ for ξ_c. Using Eq. (13), one can determine the phase $\Phi(r_0)$ that must be programmed into the SLM to produce the desired caustic SoR $r_c(\xi_c)$.

A characteristic case is that of a power-law phase $q(r)$ which leads to a power-law caustic also. Setting $q(r) = br^n$ and eliminating r_0 from Eqs. (11), the equation of the caustic $r_c(\xi_c)$ reads

$$r_c = f\left[a - d\left(\xi_c / f^2 \right)^{\nu} \right], \tag{14}$$

where $d = \nu^{-1}\left[n(n-1)b \right]^{1-\nu}$, $\nu = (n-1)/(n-2)$ and $\xi_c > 0$. For $n > 2$, we have $\nu > 1$, and hence a convex caustic SoR with a waist that starts from a maximum $2af$ at $\xi_c = 0$ to vanish on axis at $\xi_c = f^2 (a/d)^{1/\nu} \triangleq L$. As was shown in [6], the point $\xi_c = L$, at which the caustic collapses, is an inflection point for the wave amplitude, i.e. a point where the amplitude gradient along the beam axis has a local maximum. Being very close to the focus, this point also determines approximately the distance between the image plane and the target. Therefore the range of the beam and its maximum waist size can be adjusted through the lens' focal length f, which is one of

the advantages of the FT approach, as mentioned in the introduction. Equation (14) also shows that, for a given power ν, a larger *b*, i.e. a stronger nonlinear phase modulation, results in a smaller *d*, i.e. a weaker accelerating caustic. This is a rather counter-intuitive property stemming from the FT relation between object and image waves. Also counter-intuitively, the order of the caustic *v* is a decreasing function of the order *n* of the nonlinear phase term; as a result, the required phase for higher-power caustics $(\nu = 3,4,5,...)$ is of sub-cubic order $(n = 5/2, 7/3, 9/4, ...)$.

Here we would like to comment on the role of the linear phase component in Eq. (1). As indicated by Eqs. (6) and (14), this term is responsible for the formation of the dark disk on the image plane. Indeed, in the absence of $q(r)$, the problem reduces to Fourier-transforming a wave with a linear radial phase, a situation encountered when, for example, working with Bessel beams. In this case, no caustic is formed, but rather all rays leave the object plane in parallel and are focused by the lens on a circle on the image plane where a thin bright annulus appears (a circle for idealized Bessel beams). The inclusion of the nonlinear phase component subtly disturbs this perfect ray focusing, in such a way that a smooth convex caustic is formed and the AAF phenomenon is generated. The single bright annulus on the image plane then transforms to the pattern of concentric Airy rings. In conclusion, the linear term is needed to obtain a circular focusing pattern which the disturbance of the nonlinear phase transforms to a CAB-like pattern that evolves into an AAF wave. A closed-form approximation of the beam amplitude close and exactly on the caustic SoR can be obtained by a SP computation of the Fresnel integral of Eq. (7). As happens in other families of AAF waves [6], the field near the caustic is contributed by two close stationary points on the input plane $(z = 0)$, which collapse into a single second-order stationary point when the field is observed exactly on the caustic. The result is an Airy amplitude profile. The same method can be used to find the field at the focus, which is now contributed by a continuum of points lying on a circle on the input plane. In the Appendix an outline is given of how analytical expressions for the field in different regions can be obtained.

Returning to Eq. (14), it interesting to note that AAF beams with parabolic caustics $(\nu = 2)$ require the input wavefront to be modulated with a cubic phase $(n = 3)$. This is not a surprise if one takes into account our recent analytical results on the FT of CABs [7]. In this work, the FT (expressed as a Hankel transform) of the

CAB $Ai(R-r)$, was found to behave as $B(k)J_0\left(kR+k^3/3\right)$, where $B(k)$ is a complicated super-Gaussian envelope. From the asymptotic behaviour of Bessel function, it follows that, for large k, the FT behaves proportionally to $\cos\left(kR+k^3/3\right)$, i.e. as a real envelope modulated with a cubic phase. Hence, from the viewpoint of present work, the parabolic body of a CAB is a by-product of the cubic phase modulation of its spectrum, which can be considered as the analogue of the same FT property of 1D Airy beams [3].

The caustic SoR of Eq. (14) develops in the half-space $z>2f$ and the generated beam is AAF with its focus occurring on axis shortly after $z=2f+L.$ This is a result of the phase modulation in Eq. (1) being of diverging nature. If instead, the complex conjugate initial condition $u_0^*(r)$ is assumed (converging phase modulation), then the entire field in the half-space behind the lens becomes $-u^*(4f-z)$, i.e. it is mirrored with respect to the focal plane and the mirror-symmetric of Eq. (14) caustic is formed in $f<z<2f$. Moreover, as a result of the converging phase modulation itself, another caustic SoR is formed before the lens $(z<f)$, having the expression $r_c=z\left(dz^{-\nu}-a\right)$. This caustic is asymptotic (varies as $z^{1-\nu}$) to the input plane and, after passing through the lens, it experiences an inward slope discontinuity and transforms into a power-law caustic. If additionally the beam parameters are chosen so that $L<f \Leftrightarrow d>af^{\nu}$, then the transmitted power-law caustic collapses at $z=2f-L$, a point of maximum but negative amplitude gradient, thus imparting to the transmitted beam a AADF character. In the spirit of our previous work [7], we term this condition as the *weak-chirp* regime. On the other hand, when $L>f \Leftrightarrow d<af^{\nu}$, the chirp is strong enough to make the caustic collapse before the lens at $z=(d/a)^{1/\nu}$ and no focus occurs after the lens.

As shown in [7], if the input amplitude is properly engineered, the generated CAB can have two foci, the first being AADF and the second AAF. As a result, an elegant, perfectly mirror-symmetric optical bottle is formed between the two foci which can be used as an optical trap. Optical bottles can also be built by the approach presented here, however with some additional effort by letting the input beams $\mathrm{u}_0(\mathrm{r})$

and $\mathrm{u}_0^*(\mathrm{r})$ interfere in a standing wave pattern of the form $A(r)\cos[\Phi(r)]$. In that case each of the two components creates half of the full caustic. The parameters should, of course, be tuned in the weak-chirp regime, so that the bottle lies entirely behind the lens. An illustrative example is given in the next Section for an optical bottle with sinusoidal shape.

3. Numerical Examples

To illustrate our analytical arguments, we devote this Section to numerical simulations. Note that, in all of the following figures, the spatial coordinates are normalized. To give a sense of the beam's actual extent, typical values for the length scales can be $x_0 = 50\,\mu m$ in the transverse and $2\pi x_0^2/\lambda = \pi\, cm$ in the longitudinal direction, at a wavelength around $\lambda = 500\, nm$.

Let us first demonstrate the AAF and AADF mechanisms through the ray optics picture. Figure 2(a) presents the results of ray tracing for a wave with the phase modulation of Eq. (1) and the parameters $n = 3,\ a = 1,\ b = 1/3000,$ being Fourier-transformed by a lens with $f = 10$ (also in $2\pi x_0^2/\lambda$ units). The chirp parameter has been chosen to satisfy $b = 1/\left(3f^3\right),$ resulting in the formation of the parabolic caustic $r_c = 10 - \xi_c^2/4,$ (indicated with a dashed curve) which is familiar from 1D Airy beams [3]. In Fig. 2(b), the corresponding ray pattern is depicted for a beam with the same parameters but with the complex conjugate input amplitude. Note how the exactly symmetric caustic now develops in $f < z < 2f,$ and also the caustic $r_c = z\left(250z^{-2} - 1\right)$ developing in $0 < z < f.$ The two curves meet at the lens' plane with different slopes, as a result of the lens' focusing action.

Wave simulations of the two previous configurations are shown in Fig. 3 and 4, respectively, as obtained by numerically solving the paraxial equation of propagation. In both cases the envelope of the input beam has been assumed to be the Gaussian $\mathrm{A}(r) = \exp\left(-r^2/45^2\right)$. The results clearly verify our expectations from the ray-optics approach. In Fig. 3(a), the wave initially expands due to the diverging phase modulation; however, after passing through the lens, it starts to converge and it eventually forms an evident caustic SoR beyond the image plane. The superposed

analytical curve of Eq. (14), drawn with a dashed line, confirms the expected parabolic profile of this caustic. Figure 3(b) depicts the maximum intensity over the transverse plane versus the propagation distance in logarithmic scale. The onset of the AAF phase is signified by an evident *knee* in the $I_{\max}$ curve (indicated with an arrow) that occurs at $z \simeq 25.8$. Shortly after, at $z = 2f + L \simeq 26.3$, the caustic collapses and the wave amplitude $\left(I_{max}^{1/2}\right)$ has an inflection point, i.e. its gradient is maximum. The abruptness of focusing can be appreciated by the jump in the rate of increase of $log\left(I_{max}\right)$ which is averagely 0.22 (per z unit length) before and 2.3 after the knee. A reversed, defocusing behavior is obtained in Fig. 4, where the opposite phase modulation has been applied on the same Gaussian wavefront. Now the wave before the lens converges and forms a caustic that is well fitted by the equation $r_c = z(250z^{-2} - 1)$ (dashed line), that was predicted by ray-optics. Passing through the lens, this caustic experiences an inward slope discontinuity and transforms into the part of the parabola $r_c = 10 - \xi_c^2 / 4$ for $\xi_c < 0$. As this caustic SoR contracts, I_{max}, shown in Fig. 4(b), exhibits a series of maxima with gradually increasing strength. The last maximum, located at $z \simeq 13.4$, signifies the onset of the AADF phase that continues up $z \simeq 14.2$ with a large negative slope for $log\left(I_{max}\right)$ around -2.3 in average. At this point the I_{max} curve has a knee (indicated by an arrow), that introduces a phase of slow defocusing with a slope -0.22 for $log\left(I_{max}\right)$. Between the maximum and the knee, an inflection point occurs at $z \simeq 13.7$ as a result of the collapse of the caustic. The caustic extends up to the focal plane, beyond which the wave is completely diffracted.

As another example, we wish to produce an optical bottle beam with the sinusoidal caustic $r_c = af\cos(\kappa\xi_c)$. Parameter κ determines the length of the bottle along the z axis, i.e. approximately π / κ. Inserting this equation into Eq. (13) and completing the algebra, the required phase is

$$\Phi(\mathrm{r}) = \frac{\kappa \mathrm{a}^2 \mathrm{f}^2}{4}\left[\left(2\mathrm{x}^2 + 1\right) sin^{-1}(\mathrm{x}) + 3\mathrm{x}\sqrt{1 - \mathrm{x}^2}\right], \tag{15}$$

where $\mathrm{x} = \mathrm{r} / \left(\kappa \mathrm{af}^2\right)$ is a normalized radius. Expression (15) is valid for $x \le 1$, i.e. for points on the input plane with $r \le \kappa a f^2$. Rays emitted from that disk create the half-

period of the sinusoidal caustic $(|\xi_c| \le \pi/2\kappa)$. For $r > \kappa a f^2$, $\Phi(\mathrm{r})$ is chosen so that the caustic is continued smoothly for $|\xi_c| > \pi/2\kappa$. Among infinite possibilities, we here opt for a parabolic continuation, which is expressed by $r_c = (af/4\pi)\left(\pi^2 - 4\kappa^2\xi_c^2\right)$. Substituting again into Eq. (13), the corresponding extension of the phase is found

$$\Phi(\mathrm{r}) = \frac{\kappa a^2 f^2 \pi}{24}\left(2\mathrm{x}^3 + 6\mathrm{x} + 1\right), \quad \mathrm{x} > 1. \tag{16}$$

Figure 5 shows the simulation results for the parameters $\kappa = \pi/12$, $a = 1$, $f = 10$. The input amplitude is the standing wave $u_0(r) = \exp[-(r/45)^2]\cos[\Phi(r)]$ that is needed to form the complete caustic. The results verify the formation of the optical bottle with a shape that agrees well with the superposed sinusoidal curve (Fig. 5(a)). In the $I_{max}(z)$ curve of Fig. 5(b), the AADF and AAF phases defining the ends of the bottle are evident. Notice also in the inset of the same figure the characteristic Airy-like pattern of concentric rings developing on the image plane.

We conclude by noting that the proposed FT method is perfectly applicable for producing accelerating 1D or 2D beams with pre-engineered trajectories. Indeed, the results of Section 2 are valid for (1+1)D beams evolving in Cartesian coordinates *x*-*z* and being Fourier transformed by a cylindrical lens. Then, in analogy to Eq. (1), the 1D input condition is $u_0(x) = A(x)\exp[i\Phi(x)]$, where the phase modulation now reads

$$\Phi(x) = ax + q(x), \tag{17}$$

with x running from $-\infty$ to $+\infty$. For a given function q, the equation of the 1D caustic is again found from Eq. (11), replacing r_c with x_c and r_0 with x_0, and $s_0(x_0) = \Phi'(x_0)$ in analogy to Eq. (8). Inversely, for a desired caustic $x_c(\xi_c)$, the required phase is found from Eq. (13) with the same substitutions. For example, one finds that, in order to produce the power-law caustic of Eq. (14), the nonlinear phase term should be $q(x) = sgn(x)b|x|^n$, where $\mathrm{sgn}(x)$ is the sign function. The linear term (ax) can now be freely tuned, and even be negative or zero, to shift the beam

laterally. An example is shown in Fig. 6(b) for a configuration with the parameters $n = 5/2,\quad a = 0,\quad b = 0.00253,\quad f = 10$ and the Gaussian envelope $\mathrm{A}(x) = \exp[-(x/45)^2]$. The resulting 1D beam trajectory agrees very well with the superposed third-order caustic $r_c = -\xi_c^3/27$. Note also in the corresponding ray tracing result of Fig. 6(b) that the two symmetric parts of the caustic, before and after the image plane, are formed by rays emitted from half-planes $x < 0$ and $x > 0$ of the input wavefront, respectively.

Using separation of variables, the above can be readily generalized in 2D beams. For example, the beam with input amplitude $u_0(x,y) = A(x)\,A(y)\exp\left[i\Phi(x) + i\Phi(y)\right]$, will produce a caustic that accelerates along the $x = y$ direction. An example is shown in Fig. 7, for the envelope and phase functions of the previous example.

4. Conclusions

We have proposed a simple yet general method for producing in the Fourier space AAF and AADF optical beams with arbitrary convex caustic SoR. The method involves the radial modulation of a simple optical wavefront with an appropriately designed nonlinear phase structure and subsequently a FT operation by means of a lens. The required phase is the sum of a linear and a nonlinear term, with the second being responsible for the shape of the caustic. Through both wave and ray optics we showed how arbitrary power-law caustics can result from a power-law nonlinear phase component. In particular for second-order caustics, we realized that the parabolic shape is a result of the cubic phase modulation of the beam's spectrum, a conclusion that we have previously reached specifically for CABs.

The FT method proposed here is expected to offer certain advantages over the direct generation of AAF beams using phase masks only, such as the ability to easily control the size and range of the produced beams through the lens' focal strength. In addition perfectly symmetric optical bottles can be created and scaled at will. Our procedure can also be used for producing 1D or 2D beams with arbitrary convex caustics, thus providing a versatile tool for all kinds of accelerating waves.

5. Acknowledgement

This work was supported by the FP7-REGPOT-2009-1 project "Archimedes Center for Modeling, Analysis and Computation (ACMAC)", by the United States Air Force Office of Scientific Research (USAFOSR-grant nos. FA9550-10-1-0561 and FA9550-09-1-0474) and by the National Science Foundation (PHY-0800972).

6. Appendix

Here we briefly outline how the field amplitude of the AAF wave can be approximately derived in analytic form. Referring to Fig. 2(a), the field beyond the image plane $(\xi > 0)$ is written

$$u(r,\xi) = \frac{1}{i\xi}\int_0^{+\infty} u(\rho,\xi=0)\exp\left(i\frac{\rho^2+r^2}{2\xi}\right)J_0\left(\frac{\rho r}{\xi}\right)\rho d\rho, \tag{A1}$$

where the field on the image plane is given by Eq. (2). As implied by Eq. (7), the latter field can be expressed as an envelope modulated with a nonlinear phase

$$u(\rho,\xi=0) = \mathrm{B}(\rho)\exp[-iQ(\rho)], \tag{A2}$$

with the negative sign of the phase indicating focusing. For AAF waves with power-law caustics, the phase is of the form $Q(\rho) \propto (\rho - af)^{\beta}$, with $1 < \beta < 2$, as can be deduced from Eq. (7). Since the above integral cannot be computed analytically, a SP approximation is usually employed. From the ray tracing result of Fig. 2(a) it can be shown that one must distinguish between four regions which are defined from the caustic SoR and the cylinder $r = af$. The regions are shown in Fig. 8. In region #1, which lies in $r > af$ and outside the caustic SoR, the field at each point is contributed by a single ray. In region #2, which lies in $r < af$ and outside the caustic SoR, two rays meet at each point. In region #3, which lies in $r > af$ and inside the caustic SoR, three rays meet at each point (one coming from the right and two from the left half-plane). Finally, in region #4, lying in $r < af$ and inside the caustic SoR, four rays (two from either side) contribute to the field observed at each point. The above are valid off axis. On axis a continuum of rays, emerging from a circle (on focus) or two

circles (off focus), intersect at each point and a different approach is applicable, as explained in the following.

Now let us see what is the appropriate numerical treatment for each region. In regions #1, #3 where $r > af$, the argument of J_0 in Eq. (A1) is large enough to yield oscillations. Then one substitutes Eq. (4) into Eq. (A1), also using also used Eq. (A2), to obtain the double integral

$$u(r,\xi) = \frac{1}{i2\pi\xi}\int_0^{+\infty}\int_0^{2\pi} \mathrm{B}(\rho)\exp\left(i\frac{\rho^2 + r^2 - 2\rho r\cos\varphi}{2\xi} - iQ(\rho)\right)\rho d\rho d\varphi, \qquad \text{(A3)}$$

which is subsequently treated with the SP method for two variables. The stationarity conditions $Q'(\rho) = (\rho \mp r)/\xi,$ and $\varphi = 0, \pi,$ have one solution $(\rho_1, 0)$ in region #1 and three solutions $(\rho_1, 0), (\rho_{2,3}, \pi)$ in region #3.

The above approach can also be applied in regions #2 and #4, provided that the point is not too close to the axis. Note also that, in region #2, as the caustic is approached before its collapse, the two first-order stationary points merge to a second-order one and a third-order expansion of the phase leads to the familiar Airy dependence of the field amplitude (the 'fold' using terminology of catastrophe theory). Note that such an expansion is always possible since $Q'''(\rho) \propto (\rho - af)^{\beta-3}$ with $\beta < 2,$ hence the third derivative of the phase is never zero.

Finally, for points near and exactly on axis, the Bessel function factor in Eq. (A1) varies slowly and can be absorbed in the envelope. Then one can apply the standard SP method to the integral

$$u(r,\xi) = \frac{1}{i\xi}\int_0^{+\infty} \mathrm{B}(\rho)J_0\left(\frac{\rho r}{\xi}\right)\exp\left(i\frac{\rho^2 + r^2}{2\xi} - iQ(\rho)\right)\rho d\rho, \qquad \text{(A4)}$$

as was done in [6]. The stationarity condition $Q'(\rho) = \rho/\xi$ yields two first-order stationary points which merge into a second-order one as the collapse point (the caustic) is approached from above. By third-order expanding the phase, one again finds that the on-axis amplitude near the focus is proportional to an Airy function.

References

1. N. K. Efremidis, D. N. Christodoulides, "Abruptly autofocusing waves," Opt. Lett., vol. 35, no. 23, pp. 4045-4047, 2010.
2. G. A. Siviloglou and D. N. Christodoulides, "Accelerating finite energy Airy beams," Opt. Lett. 32, 979-981 (2007).
3. G. A. Siviloglou, J. Broky, A. Dogariu, and D. N. Christodoulides, "Observation of Accelerating Airy Beams," Opt. Lett., vol. 32, pp. 979-981 (2007).
4. D. G. Papazoglou, N. K. Efremidis, D. N. Christodoulides, and S. Tzortzakis, "Observation of abruptly autofocusing waves," Opt. Lett. 36, 1842-1844 (2011).
5. P. Zhang, J. Prakash, Ze Zhang, M. S. Mills, N. Efremidis, D. Christodoulides, and Z. Chen, "Trapping and guiding microparticles with morphing autofocusing Airy beams", Opt. Lett., vol. 36, no. 15, pp. 2883-2885 (2011)
6. I. Chremmos, N. K. Efremidis, D. N. Christodoulides, "Pre-engineered abruptly autofocusing beams," Opt. Lett., vol. 36, no. 10, pp. 1890-1892, 2011.
7. I. Chremmos, P. Zhang, J. Prakash, N. K. Efremidis, D. N. Christodoulides, and Z. Chen: Fourier-space generation of abruptly autofocusing beams and optical bottle beams, Opt. Lett., vol. 36, no. 18, pp. 3675-3677, 2011.
8. G. A. Siviloglou, J. Broky, A. Dogariu, and D. N. Christodoulides, "Observation of accelerating Airy beams," Opt. Lett. 32, 979-981 (2007).
9. E. Greenfield, M. Segev, W. Walasik, and O. Raz, "Accelerating light beams along arbitrary convex trajectories," Phys. Rev. Lett. 106, (21), 213902 (2011).
10. L. Froehly, F. Courvoisier, A. Mathis, M. Jacquot, L. Furfaro, R. Giust, P. A. Lacourt, J. M. Dudley: Arbitrary accelerating micron-scale caustic beams in two and three dimensions. Opt. Express, vol. 19, no. 17, pp. 16455-16465, August 2011.
11. L. Felsen, N. Marcuvitz: *Radiation and Scattering of Waves*, (Wiley-IEEE Press 1994)

Figures

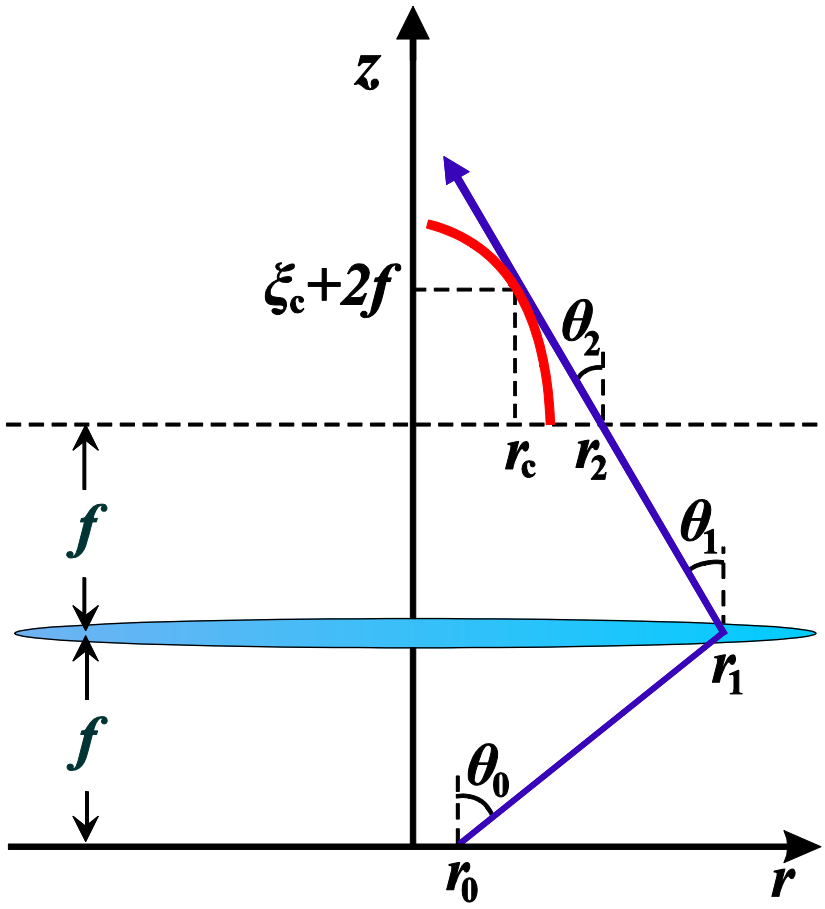

Figure 1: (Color online) Schematic of a ray travelling through a single-lens FT system. The lens is positioned at $z = f$. The red (convex) curve indicates the caustic formed beyond $z = 2f$.

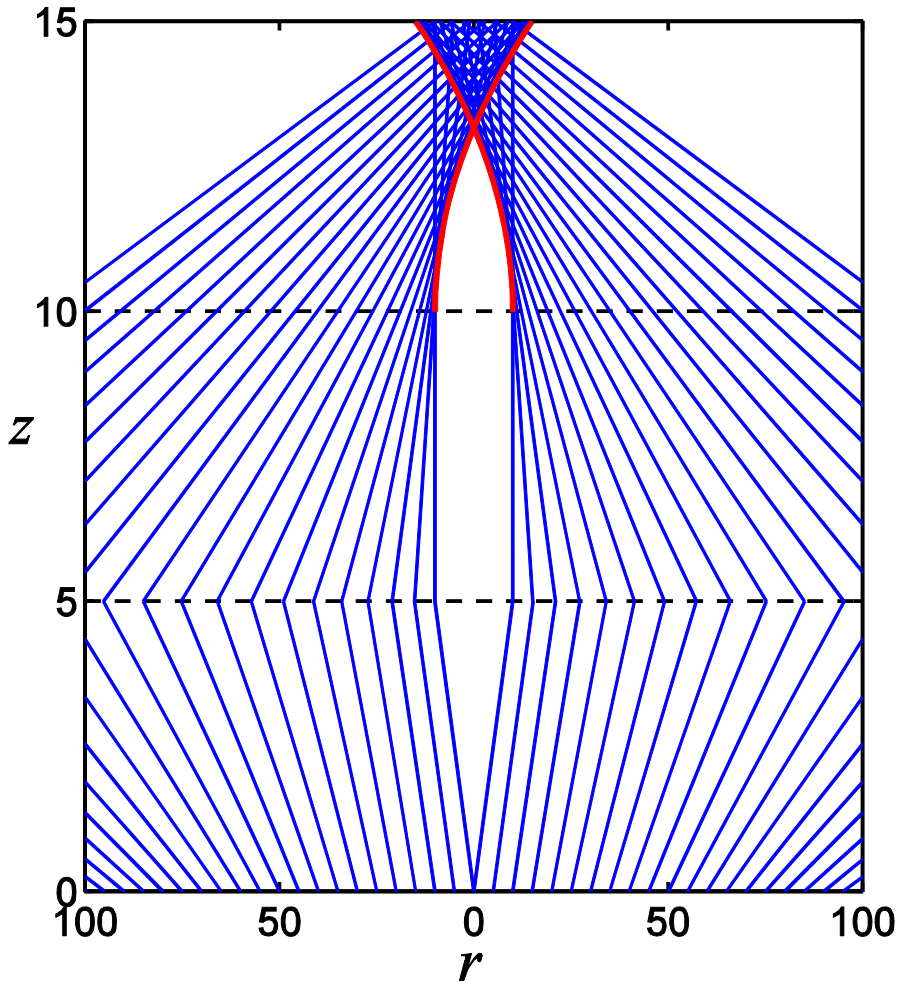

(a)

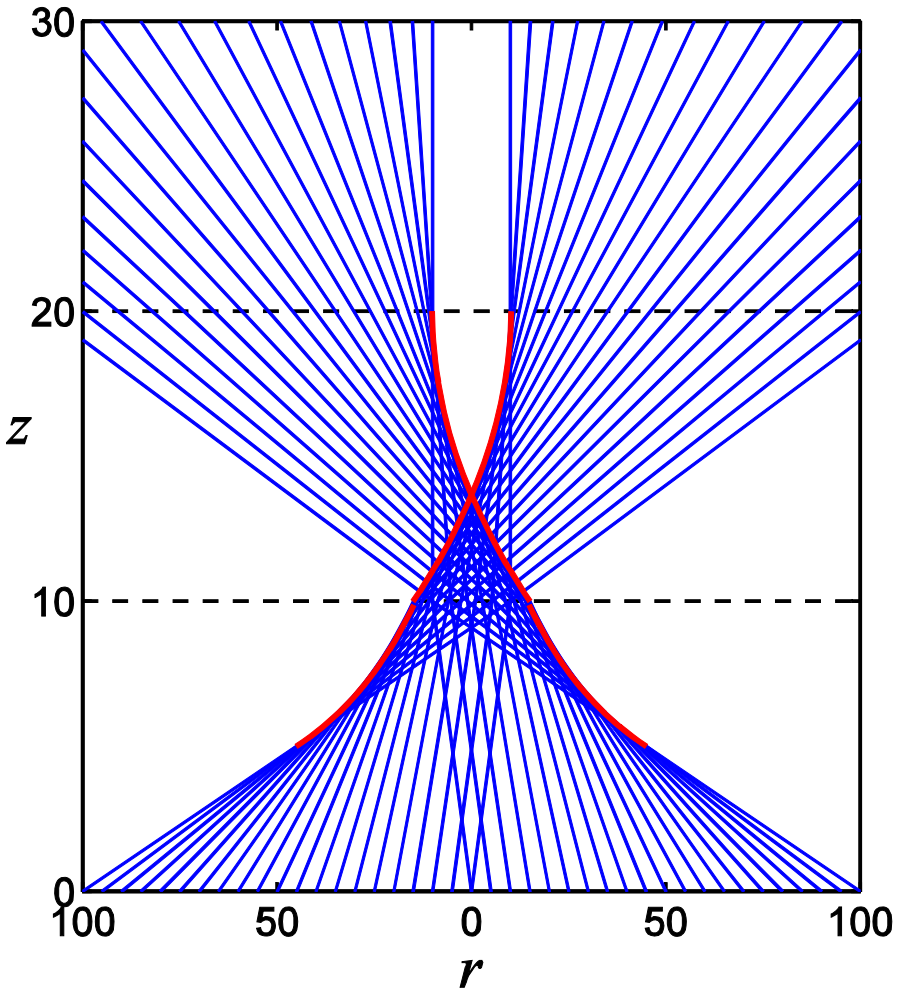

(b)

Figure 2: (Color online) Ray patterns on a vertical plane for a beam with input phase: a) $\alpha r + br^n$ and b) $-\alpha r - br^n$, with parameters $n = 3$, $a = 1$, $b = 1/3000$, and a lens with $f = 10$. The red curves (ray envelopes) are the caustics, while the dashed horizontal lines indicate the lens' plane $(z = f)$ and the image plane $(z = 2f)$.

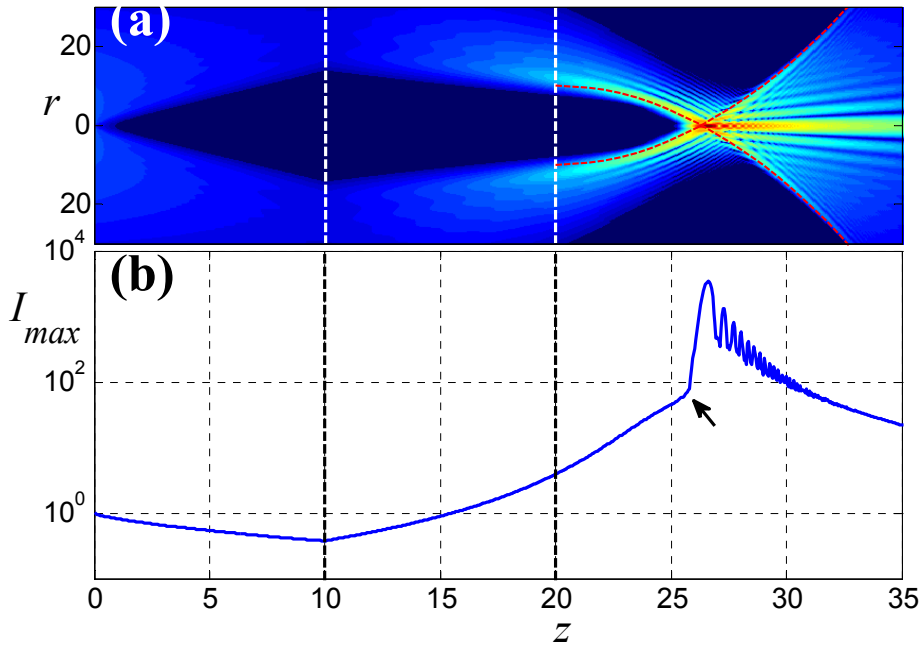

Figure 3: (Color online) (a) Amplitude evolution of a beam with Gaussian input envelope with e^{-1} radius $w \simeq 45$ and the phase modulation parameters of Fig. 2(a). The dashed curves are the caustics of Eq. (11). (b) Maximum intensity versus propagation distance. The arrow indicates the point where the AAF starts. The dashed vertical lines indicate planes $z = f$ and $z = 2f$.

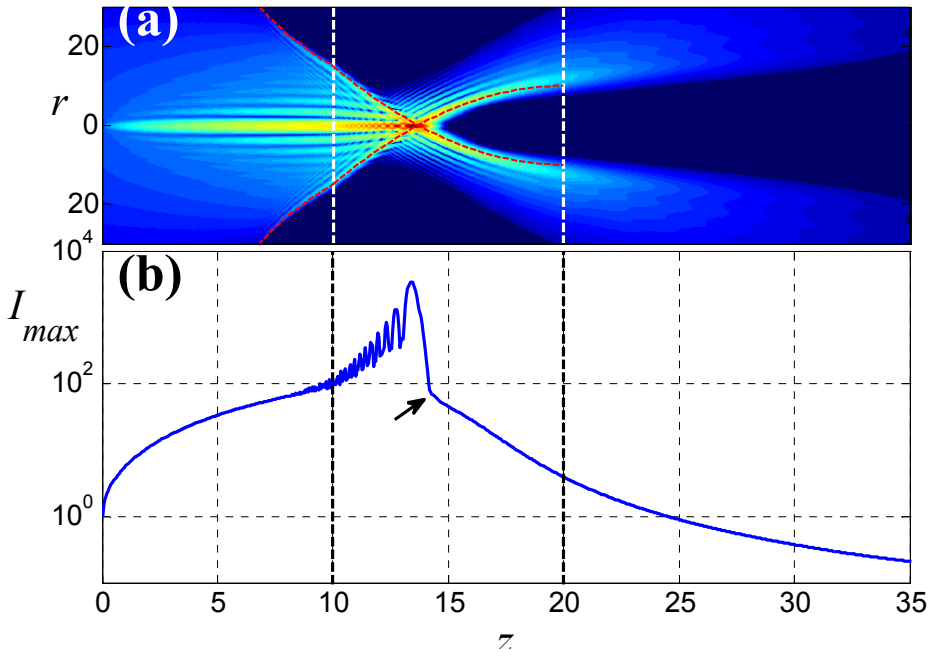

Figure 4: (Color online) (a) Amplitude evolution of a beam with the same parameters with Fig. 3 but with the complex conjugate input amplitude. The dashed curves indicate the caustics. (b) Maximum intensity versus propagation distance. The arrow indicates the point where the AADF ends. The dashed vertical lines indicate planes $z = f$ and $z = 2f$.

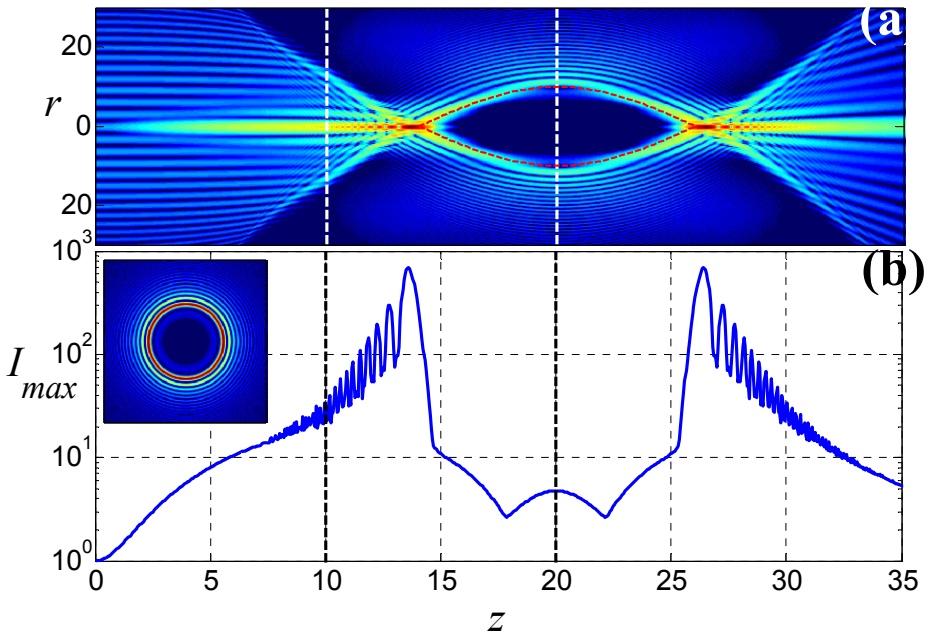

Figure 5: (Color online) (a) Amplitude evolution of a beam with input amplitude $\exp[-(r/45)^2]\cos[\Phi(r)]$, where Φ is given by Eqs. (14),(15) for $\kappa = \pi/12$, $a = 1$, $f = 10$. The dashed curves indicate the sinusoidal part of the caustic. (b) Maximum intensity versus propagation distance. The dashed vertical lines indicate planes $z = f$ and $z = 2f$. The inset shows the amplitude distribution on the image plane.

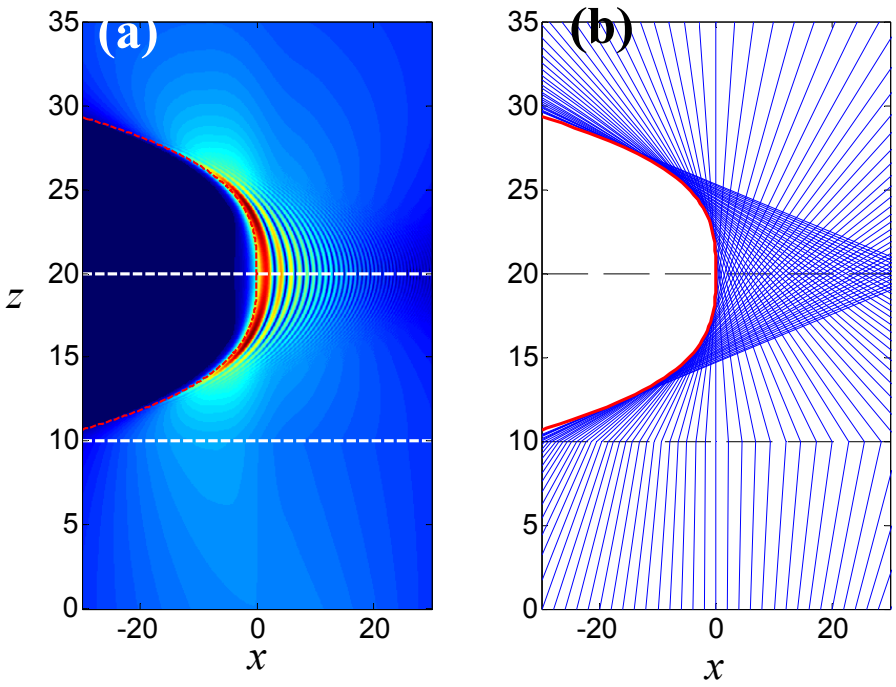

Figure 6: (Color online) (a) Amplitude evolution of a 1D beam with parameters $n = 5/2,\ a = 0,\ b = 0.00253,$ a Gaussian input envelope with e^{-1} width 90 and a lens with $f = 10.$ The envelope curve is the caustic, while the dashed horizontal lines indicate the lens and image planes. (b) Corresponding ray pattern.

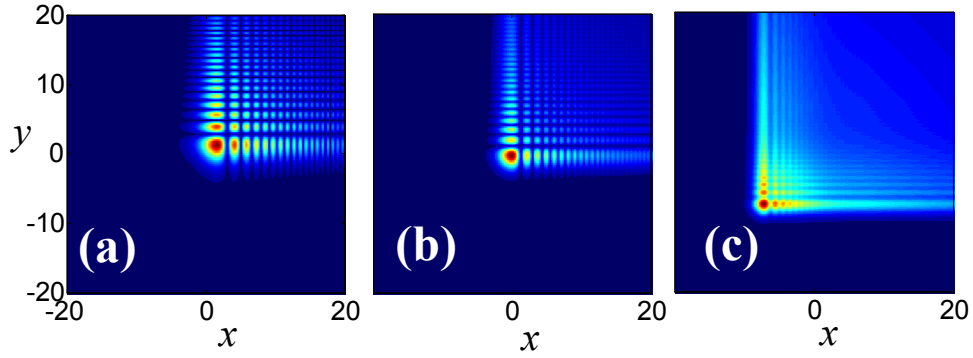

Figure 7: (Color online) Transverse amplitude at different z-planes of an accelerating 2D beam produced by Fourier-transforming the input wavefront $u_0(x,y) = A(x)\,A(y)\exp\left[i\Phi(x) + i\Phi(y)\right]$, with $\mathrm{A}(u) = \exp[-(u/45)^2]$ and $\Phi(u) = 0.00253\,sgn(u)\,|u|^{5/2}$. (a) z=20, (b) z=23, (c) z=26. The lens has $f = 10$.

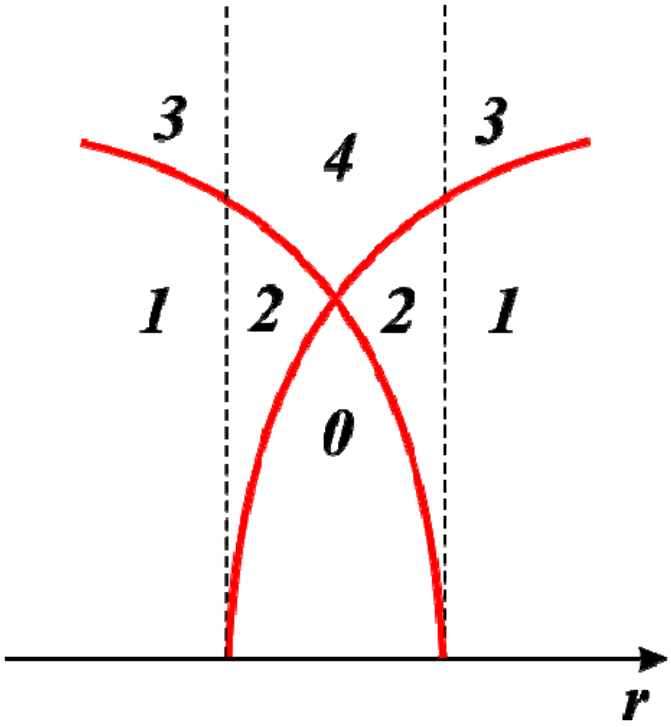

Figure 8: Regions for ray optics computations of the field of an AAF wave. The regions are characterized by the number of rays contributing to the field at any point.